

Quasiparticle Description of the QCD Plasma, Comparison with Lattice Results at Finite T and μ

K. K. Szabó and A. I. Tóth

*Institute for Theoretical Physics, Eötvös University, Pázmány 1, H-1117 Budapest,
Hungary*

ABSTRACT: We compare our 2+1 flavor, staggered QCD lattice results with a quasiparticle picture. We determine the pressure, the energy density, the baryon density, the speed of sound and the thermal masses as a function of T and μ_B . For the available thermodynamic quantities the difference is a few percent between the results of the two approaches. We also give the phase diagram on the μ_B - T plane and estimate the critical chemical potential at vanishing temperature.

Contents

1. Introduction	1
2. Quasiparticle model	2
3. Comparison with lattice results	4
4. Conclusion	11

1. Introduction

QCD at high temperatures (T) and/or quark chemical potentials (μ) plays an important role in particle physics, since it describes relevant features of nature in extreme conditions. According to the standard picture of QCD, at high T and/or μ there is a change from a state dominated by hadrons to a state dominated by partons (quarks and gluons). This transition happened in the early Universe (at essentially vanishing net baryon density [1]) and probably happens in heavy ion collisions (at moderate but non-vanishing density) and in neutron stars (at large density, for which a rich phase structure is conjectured [2, 3, 4]). There has been several studies in order to determine the thermodynamic properties of the QCD plasma. The weak coupling expansion of thermodynamic quantities shows a poor convergence near the transition temperature [5, 6, 7]. Better convergence is expected from different improved techniques, e.g. screened perturbation theory [8, 9], or a systematic rearrangement of the perturbative expansion [10], or using an effective field theory in 3D [11]. Note that noticeable deviations ($\approx 10\%$) from the ideal gas limit is expected upto temperatures as high as 1000 times the critical temperature (T_c). The lattice approach is applicable to investigate the plasma upto a several times T_c and at zero chemical potential [12, 13, 14]. The phenomenology of these lattice results has been widely analyzed in the literature. Successful quasiparticle descriptions [15, 16, 17] have been introduced to reproduce the properties of the QCD plasma. One can extrapolate these $\mu = 0$ results to non-zero baryon densities by using the thermodynamical consistency of the model. Unfortunately, until recently it was not possible to compare the $\mu \neq 0$ predictions of the quasiparticle model with direct lattice calculations. The lack of $\mu \neq 0$ lattice results was a consequence of the sign problem. The fermionic determinant in the path integral becomes complex for non-vanishing μ -s. This fact spoils any Monte-Carlo based technique used in numerical simulations.

Many suggestions were studied in detail to solve the sign problem and to give physical answers on the lattice at non-vanishing chemical potentials. Unfortunately, until recently none of them were successful. Recent interest in this field was initiated by the overlap improving multi-parameter reweighting method [18]. The phase diagram and the critical point were determined in the 2 + 1 flavor QCD on $N_t = 4$ lattices with staggered quarks [19]. Several groups confirmed the results of Refs. [18, 19] on the phase diagram [20, 21, 22]. Furthermore, it became possible to determine the equation of state (EoS) at finite chemical potentials [23], too (for a recent review on lattice QCD at non-vanishing chemical potentials see Ref. [24]). Thus, it would be of interest to see how these new lattice results can be described with the quasiparticle approach. This is the primary goal of the present paper.

The paper is organized as follows. In Section 2 we briefly summarize the quasiparticle approach at $\mu = 0$ and show how to extend it to non-vanishing chemical potentials. Section 3 compares our most recent lattice results with the prediction of the quasiparticle model. In Section 4 we summarize.

2. Quasiparticle model

In order to be self-contained we start with a brief review of the quasiparticle model¹ suggested in Ref. [16]. Consider a QCD plasma containing gluons (g), N_l number of “light” and N_h number of “heavy” quarks (l and h , respectively). These basic constituents have temperature and chemical potential dependent effective masses

$$m_i^2(T, \mu_i) = m_{0i}^2 + \Pi_i^*(T, \mu_i), \quad i = g, l, h, \quad (2.1)$$

where the m_{0i} -s are the rest masses, μ_i -s are the chemical potentials of partons and the Π_i^* -s are the asymptotic values of the hard thermal/density-loop self-energies

$$\Pi_q^* = 2\omega_q(m_0 + \omega_q), \quad \omega_q^2 = \frac{N_c^2 - 1}{16N_c} \left(T^2 + \frac{\mu_i^2}{\pi^2} \right) G^2, \quad (2.2)$$

$$\Pi_g^* = \frac{1}{6} \left[\left(N_c + \frac{N_l + N_h}{2} \right) T^2 + \frac{3}{2\pi^2} \sum_q \mu_i^2 \right] G^2, \quad (2.3)$$

where G^2 is the effective gauge coupling (depending on T , μ , see below), and the summation is performed over the quark flavors (q). We are interested in the non-zero “light” quark chemical potential region therefore we set $\mu_h = 0$ for the “heavy” quarks. Note that the baryonic chemical potential is three times the “light” quark one. In our notations $\mu_l = \mu = \mu_B/3$.

The thermodynamic potential the pressure $p(T, \mu)$ contains contribution from the ideal pressure of the quasiparticles (p_i^{ID}) and from the pressure arising from their interactions ($B(T, \mu)$):

$$p(T, \mu) = \sum_i p_i^{ID}(T, \mu_i(\mu), m_i^2) - B(T, \mu). \quad (2.4)$$

¹When writing up this paper a different phenomenological approach was compared with lattice results at non-vanishing μ in Ref. [25]. The quark-gluon plasma liquid model was found to be in close agreement with our lattice data.

The ideal gas pressure is the usual Fermi or Bose integral which takes into account the antiparticles in the quark pressure, too:

$$p_q^{ID}(T, \mu) = \frac{d_q}{6\pi^2} \int_{m_q(T, \mu)}^{\infty} d\epsilon \frac{(\epsilon^2 - m_q^2)^{3/2}}{\exp[(\epsilon - \mu_i)/T] + 1} + (\mu_q \rightarrow -\mu_q), \quad (2.5)$$

$$p_g^{ID}(T, \mu) = \frac{d_g}{6\pi^2} \int_{m_g(T, \mu)}^{\infty} d\epsilon \frac{(\epsilon^2 - m_g^2)^{3/2}}{\exp(\epsilon/T) - 1}. \quad (2.6)$$

We do not fix the quark and gluon state multiplicities separately, but we demand that their ratio should be $d_g/(d_{l,h}) = 2 \cdot 8/(2 \cdot 3 \cdot N_{l,h})$. If we impose a stationarity condition [26] on the pressure then further thermodynamic quantities (such as energy density (ϵ), quark number density (n_i) and entropy density (s)) will have only quasiparticle and mean field, $B(T, \mu)$, contributions:

$$\epsilon(T, \mu) = \sum_i \epsilon_i^{ID}[T, \mu_i(\mu), m_i^2] + B(T, \mu), \quad n_i(T, \mu) = n_i^{ID}[T, \mu_i(\mu), m_i^2], \quad (2.7)$$

where n^{ID} is the ideal quark number density. The functional form of the interaction pressure, $B(T, \mu)$, follows from the above condition, too. The derivatives of $B(T, \mu)$ in T and μ directions are easily accessible quantities

$$\left. \frac{\partial B}{\partial T} \right|_{\mu} = \sum_i \frac{\partial p_i^{ID}}{\partial m_i^2} \frac{\partial \Pi_i^*}{\partial T}, \quad \left. \frac{\partial B}{\partial \mu} \right|_T = \sum_i \frac{\partial p_i^{ID}}{\partial m_i^2} \frac{\partial \Pi_i^*}{\partial \mu}, \quad (2.8)$$

so $B(T, \mu)$ can be obtained by an appropriate line integral on the (T, μ) plane.

What remains to be done is to determine the effective gauge coupling which appears in the formula of the self-energies. For vanishing chemical potentials it decreases logarithmically with increasing temperature. A renormalization group inspired parametrization is as follows:

$$G^2(T, \mu = 0) = \frac{48\pi^2}{[33 - 2(N_l + N_h)] \log(\frac{T+T_s}{T_c/\lambda})}. \quad (2.9)$$

Imposing the Maxwell-relation between the derivatives of the quark number density and entropy

$$\left. \frac{\partial s}{\partial \mu} \right|_T = \left. \frac{\partial n_l}{\partial T} \right|_{\mu} \implies \sum_i \frac{\partial s_i^{ID}}{\partial m_i^2} \frac{\partial \Pi_i^*}{\partial \mu} = \frac{\partial n_l^{ID}}{\partial m_l^2} \frac{\partial \Pi_l^*}{\partial T} \quad (2.10)$$

yields a first order, linear partial differential equation for $G^2(T, \mu)$ with straightforwardly calculable a_T, a_{μ}, b coefficients

$$a_T(T, \mu, G^2) \cdot \partial_T G^2 + a_{\mu}(T, \mu, G^2) \cdot \partial_{\mu} G^2 = b(T, \mu, G^2). \quad (2.11)$$

This differential equation should be solved with the boundary condition at $\mu = 0$ (eq. (2.9)). Thus, the quasiparticle model is unambiguously defined by using thermodynamical consistency for non-zero μ -s above the critical line ($T_c(\mu)$). Below $T_c(\mu)$ the solution of the differential equation, thus the pressure is not unique. In this region the system has hadronic degrees of freedom instead of partonic. The quasiparticle model constructed from partons loses its validity.

3. Comparison with lattice results

As we have already mentioned the sign problem of lattice QCD at finite chemical potentials spoils any Monte-Carlo method based on importance sampling. The recently proposed overlap ensuring multi-parameter reweighting method [18] enabled us to determine the EoS at non-zero temperatures and chemical potentials [23]. The simulations were carried out on $N_t = 4$ temporal and $N_s = 2N_t \dots 3N_t$ spatial extension lattices with two “light” ($m_l = 0.384T_c$) and one “heavy” ($m_h \approx T_c$) dynamical quarks. Note that the mass of the “heavy” quark corresponds approximately to the physical mass of the strange quark, whereas the mass of the “light” quarks is several times larger than the physical values for the up/down quarks. In the lattice analysis both the temperature and the baryon chemical potential covered the range upto $\mu_B \approx 3T_c$.

Our lattice calculations were done on lattices with $N_t = 4$ temporal extension. In order to help the continuum interpretation we multiply the lattice results by the dominant $T \rightarrow \infty$ correction factors between the $N_t = 4$ and the continuum case. We denote the $T \rightarrow \infty$ limit as the SB (Stefan-Boltzmann) case.

$$c_p = \frac{p^{SB}(\mu = 0, T \rightarrow \infty, \text{continuum})}{p^{SB}(\mu = 0, T \rightarrow \infty, N_t = 4)} = 0.518, \quad (3.1)$$

$$c_\mu = \frac{\Delta p^{SB}(\mu, T \rightarrow \infty, \text{continuum})}{\Delta p^{SB}(\mu, T \rightarrow \infty, N_t = 4)} = 0.446 + \mathcal{O}\left(\frac{\mu^2}{T^2}\right). \quad (3.2)$$

Note that the m dependence of these factors are suppressed in the $T \rightarrow \infty$ limit. Here Δp indicates the difference between the pressure at $\mu \neq 0$ and the pressure at $\mu = 0$. The well-known continuum expressions for the non-interacting quark gluon plasma are

$$p^{SB}(\mu = 0, T \rightarrow \infty, \text{continuum}) = [16 + 21(N_l + N_h)/2]\pi^2 T^4/90, \quad (3.3)$$

$$\Delta p^{SB}(\mu, T \rightarrow \infty, \text{continuum}) = N_l \mu^2 T^2/2 + \mathcal{O}(\mu^4). \quad (3.4)$$

Including these dominant multiplicative corrections the results might be interpreted as continuum estimates. (Clearly, the appropriate – but more CPU-consuming – way is to carry out the lattice calculations at $N_t > 4$ and perform an extrapolation to $N_t \rightarrow \infty$.)

The quasiparticle model has four free parameters: λ and T_s to determine the gauge coupling, d_g the gluon multiplicity and $B(T_c)$ the integration constant in the interaction pressure. They were used as fit parameters in order to receive the least possible difference between the thermodynamic observables measured on the lattice and the ones predicted by the quasiparticle description. In principle it is sufficient to use only the lattice results at vanishing μ in the fitting procedure since afterwards the thermodynamical consistency unambiguously defines the quasiparticle approach; but this could lead to large differences between the two types of descriptions at non-vanishing μ -s. It turned out to be more sensible to use both the $\mu = 0$ and the $\mu \neq 0$ lattice data for fitting in order to gain a better agreement between the two approaches for higher μ -s. Therefore we fitted the quasiparticle picture on the $(\epsilon - 3p)/T^4$ at $\mu = 0$ and $\Delta p/T^4$ at our highest chemical potential ($\mu_B \approx 490$ MeV) lattice results, simultaneously. The chi-square function (χ^2) was constructed by using the statistical errors of the lattice data. We constructed statistical

errors for the fit parameters, which are to give the 68.3% confidence level corresponding to the bounds of the $\Delta\chi^2 = 4.72$ interval [27]. Clearly, the parameter region according to this confidence level has a complicated shape in the four-dimensional parameter space. The quoted errors just indicate the borders of this domain. Furthermore, these errors should be taken with a grain of salt, since the constructed χ^2 functions contains no information about the systematical uncertainties of our $N_t = 4$ lattice data. We found it to be more reliable to fit on $(\epsilon - 3p)/T^4$ lattice results instead of p/T^4 at $\mu = 0$, since minimizing the χ^2 function of the pressure yielded an interaction measure without a turning-point around $1.3T_c$, which is typical of the lattice results. The best parameter values with statistical uncertainties can be found in Table 1.

λ	$10.1^{+0.9}_{-2.0}$
T_s/T_c	$-0.85^{+0.06}_{-0.02}$
d_g	$16.4^{+0.3}_{-0.2}$
$B^{1/4}(T_c)$	$174.3^{+9.2}_{-5.2}$ MeV

Table 1: The best fit parameters of the quasiparticle model to our lattice results.

Using the best fit parameters we can obtain the temperature and chemical potential dependence of several thermodynamic quantities and compare them with lattice data. Note that we use $T_c = 170$ MeV as the overall scale in the results. In formulas and figures T_c is used as the transition temperature at vanishing chemical potential, whereas $T_c(\mu_B)$ indicates the transition temperature at non-vanishing chemical potentials. We chose the chemical potential values so as to cover the characteristic μ -s occurring in the heavy ion collisions. At our smallest chemical potential value, 27 MeV, and at around 300 MeV Au+Au colliding experiments were carried out at RHIC [28, 29], whereas at 253 MeV Pb+Pb collisions took place at SPS [30].

Figures 1 and 2 show the behavior of the “interaction measure”, $(\epsilon - 3p)$, and the pressure (both normalized by T^4) at vanishing chemical potentials. Both the lattice result and the prediction of the quasiparticle approach are given. On the one hand there is a good agreement between the two techniques for $(\epsilon - 3p)$, on the other hand for the pressure one finds a larger difference. It is easy to understand the reason for that. First of all we used $(\epsilon - 3p)$ in our fitting procedure, therefore a better agreement is expected for this quantity than for p , which is a prediction of the model. Secondly, the pressure can be obtained as an integral of the interaction measure

$$\frac{p}{T^4} = \int \frac{dT}{T} \frac{\epsilon - 3p}{T^4}. \quad (3.5)$$

Differences in $(\epsilon - 3p)$ at small temperatures dominates the above integral. Though the difference between the lattice and the quasiparticle results for $(\epsilon - 3p)$ is rather small at large T one observes a 20% difference around T_c . Therefore we end up with an $\approx 10\%$ difference for p even in the large T region. There might be several explanations for the differences between the two approaches. It can be that the lattice results in the continuum

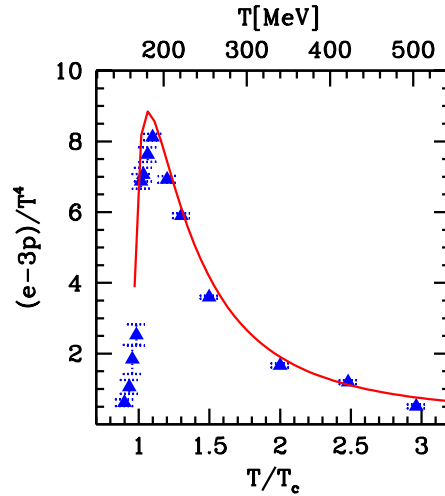


Figure 1: The interaction measure, $(\epsilon - 3p)$, normalized by T^4 as a function of T/T_c at $\mu = 0$. The line corresponds to the quasiparticle model, the points are lattice results multiplied by c_p . The errorbars show the statistical uncertainties.

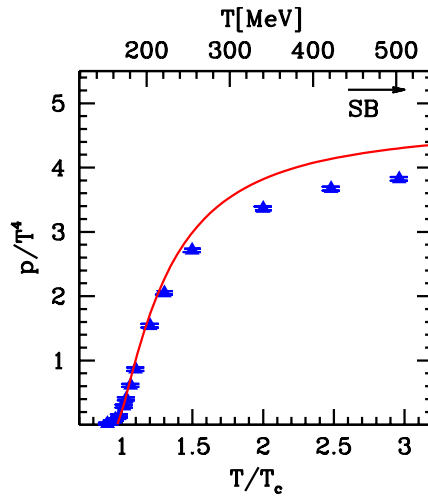


Figure 2: The pressure normalized by T^4 as a function of T/T_c at $\mu = 0$. The line corresponds to the quasiparticle model, the points are lattice results after a multiplication by c_p . The arrow indicates the high temperature ideal gas pressure of the QCD plasma (SB limit).

limit ($N_t \rightarrow \infty$) change the picture and lead to smaller discrepancies. Alternatively, it also can be that the quasiparticle approach simplifies the interaction in the quark-gluon plasma. This means that the prediction of this method can be $\approx 10\%$ off.

We show the temperature dependence of $\Delta p/T^4$ in Figure 3 and that of n_B/T^3 in Figure 4. Both figures indicate a nice agreement between the two types of QCD plasma descriptions (the largest difference is $\approx 5\%$ at low temperatures and high chemical potential). The temperature dependence of the baryon density is similar to that of the pressure

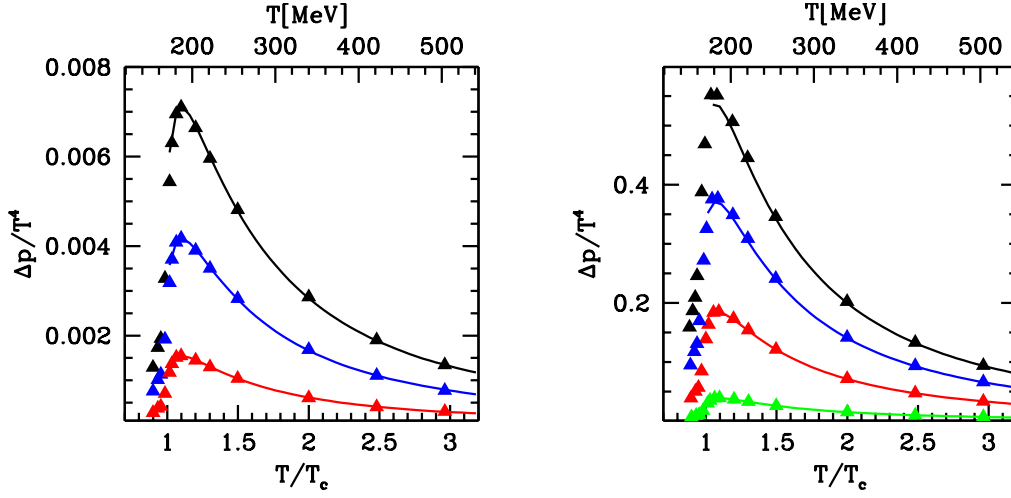


Figure 3: $\Delta p = p(\mu \neq 0, T) - p(\mu = 0, T)$ normalized by T^4 as a function of T/T_c for $\mu_B = 27, 45$ and 60 MeV in the left panel and for $\mu_B = 140, 290, 410$ and 490 MeV in the right panel (upper curves correspond to larger chemical potentials). The lines represent the quasiparticle model, the points are lattice results multiplied by c_μ . The statistical uncertainties are smaller than the point size.

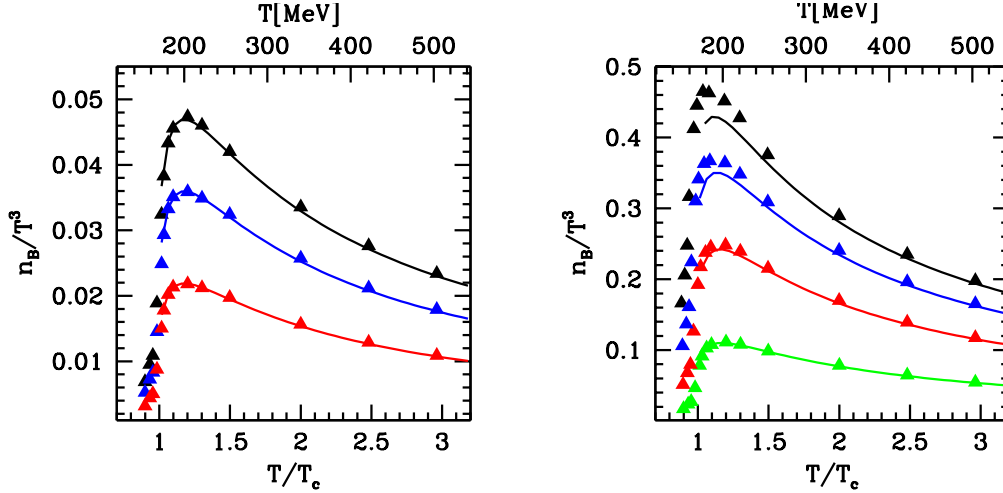


Figure 4: The baryon number density normalized by T^3 as a function of T/T_c for $\mu_B = 27, 45$ and 60 MeV in the left panel and for $\mu_B = 140, 290, 410$ and 490 MeV in the right panel (upper curves correspond to larger chemical potentials). The lines represent the quasiparticle model, the points are lattice results multiplied by c_μ . The statistical uncertainties are smaller than the point size.

since they are connected by the formula

$$T \left. \frac{\partial}{\partial \mu_B} \right|_T \left(\frac{\Delta p}{T^4} \right) = \frac{n_B}{T^3}. \quad (3.6)$$

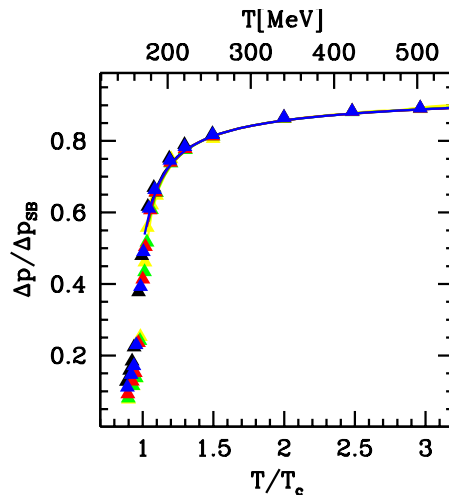


Figure 5: Δp of the interacting QCD plasma normalized by Δp^{SB} of the free gas (SB) as a function of T/T_c for $\mu_B = 60, 140, 290, 410$ and 490 MeV. The lines represent the quasiparticle model, the points are lattice results. The statistical uncertainties are smaller than the point size.

We observe an interesting scaling behavior of Δp normalized by Δp^{SB} (Figure 5). This quantity ($\Delta p/\Delta p^{SB}$) depends only on T/T_c and it is almost independent of the chemical potential. This scaling behaviour is less accurate around T/T_c and it gets more and more precise for higher temperatures.

It is of extreme importance to determine the phase line (the line, which separates the phases dominated by hadrons and partons). One is particularly interested in results at low temperatures, for which only model estimates are available. First we use the quasiparticle picture, then an extrapolation to the lattice data in order to determine the phase line.

We defined a quasiparticle critical line based on the following observation (see Figure 2): the pressure around T_c is a lot lower than the pressure at high temperatures, which is in the order of p^{SB} . A simple explanation of this fact is that the number of degrees of freedom in the QGP is much bigger than in the hadronic phase, which is a dilute gas of pions. So we set p to be a few percent of p^{SB} along the phase line (note that the result is rather insensitive to the exact value of this percentage as illustrated in Figure 6). The line defined above is depicted also at rather low temperatures and we get ≈ 1800 MeV for the point of intersection on the $T = 0$ axes. We must interpret this value as the critical chemical potential (μ_B^{crit}) with great care since for the low temperature, high chemical potential region the color-superconducting phase is conjectured [31], which is obviously not contained in this quasiparticle framework. The quasiparticle transition line shows a nice agreement with the directly measured lattice transition line in the $\mu_B < 3T_c$ region (Figure 6). Outside of this region we do not have direct lattice results. It is intriguing to see the behavior of the critical lines when $T \rightarrow 0$. We extended our lattice transition line to zero temperature by using two fits namely a second and a fourth order polynomial. Due to μ versus $-\mu$ symmetry we keep only even order terms in the fitting procedure. The bands

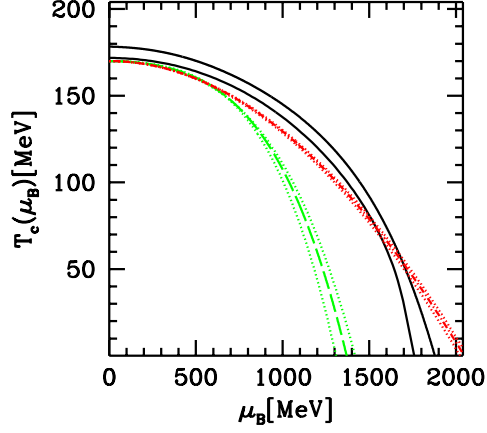


Figure 6: The critical lines on the temperature versus chemical potential plane. The solid curves are quasiparticle critical lines which were obtained with the best fit parameters. The lower curve corresponds to the pressure equals to zero criteria while the pressure equals to $0.14p^{SB}$ along the upper curve. The dashed and dashed dotted (lower and upper) lines are the extrapolations of the lattice critical line to $T = 0$ using a 4th and a 2nd order polynomial, respectively. The dotted lines show the influence of the statistical uncertainties of the lattice results. Note that our critical lines loose their validity towards higher chemical potentials, where the color superconducting phase comes into play.

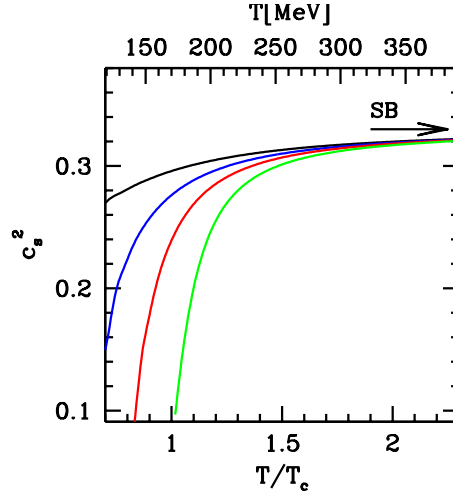


Figure 7: The speed of sound squared in the QCD plasma as a function of $T/T_c(\mu_B)$ at various chemical potentials ($\mu_B = 0, 900, 1200$ and 1500 MeV). Upper curves correspond to larger values of μ_B . The arrow indicates the speed of sound squared in the ideal gas limit $((c_s^{SB})^2 = 1/3)$.

in Figure 6 indicate the statistical uncertainties of the fits. The two curves agree nicely in the directly measured $\mu_B < 3T_c$ region. They deviate for smaller temperatures and larger chemical potentials. The quadratic polynomial fit predicts at vanishing temperature

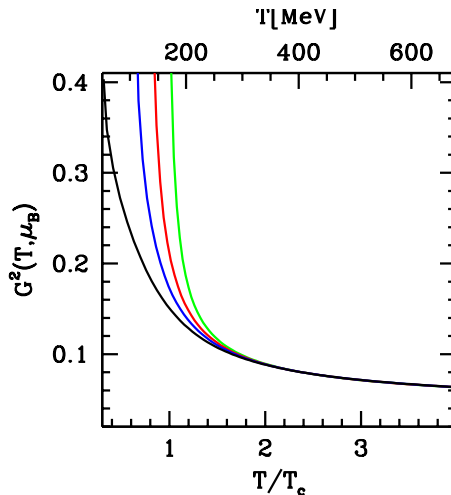


Figure 8: The coupling constant squared as a function of T/T_c for various chemical potentials ($\mu_B = 0, 900, 1200$ and 1500 MeV). Upper curves correspond to smaller values of μ_B .

$\mu_B^{\text{crit}} \approx 2000$ MeV (which exceeds expectations). The quartic approximation gives for the same quantity $\mu_B^{\text{crit}} \approx 1400$ MeV. The difference between the predictions of the two kinds of polynoms might be interpreted as a rough estimate for the systematic uncertainty of the extrapolation to low temperatures.

The dynamical properties of the plasma phase is primarily determined by the speed of sound

$$c_s^2(T, \mu_B) = \frac{dp}{d\epsilon}. \quad (3.7)$$

As it can be seen in Figure 7 increasing chemical potential yields higher speed of sound.

One can also look for the predictions of the quasiparticle model for quantities which are straightforward predictions of the quasiparticle approach however, it is difficult to obtain them directly on the lattice. Such important quantity is the gauge coupling of the quasiparticle picture, which is shown in Figure 8. Note that the static potential at finite chemical potentials can be in principle measured on the lattice. Using the lattice potential one can easily define the gauge coupling. Clearly, the parametrization of the gauge coupling in the quasiparticle picture is not equivalent with the above mentioned coupling.

In order to understand the typical degrees of freedom in the high temperature QCD phase at non-vanishing chemical potentials it is instructive to study the effective masses of the quasiparticles. Figure 9 shows the temperature dependence of the light quark masses for different chemical potentials, whereas Figure 10 presents the results on the gluon masses. According to our observations these quantities are almost independent of the chemical potential in the $\mu_B < 3T_c$ region. Due to the stationarity condition $\partial p / \partial m_i = 0$ small changes in the mass do not change the pressure. It means that the chemical potential dependence of the thermodynamic quantities are primarily coming from the direct μ_B dependence of the Fermi integrals.

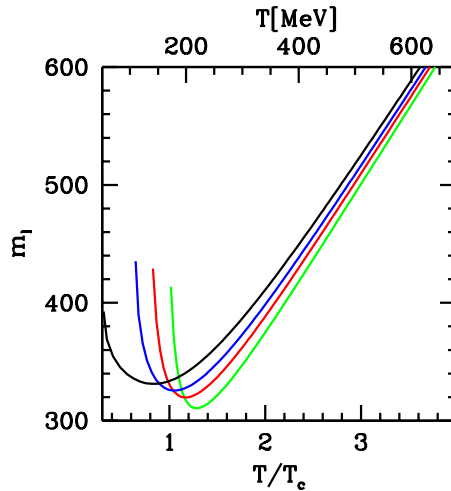


Figure 9: The effective mass of the light quarks as a function of T/T_c for various chemical potentials ($\mu_B = 0, 900, 1200$ and 1500 MeV, right to left).

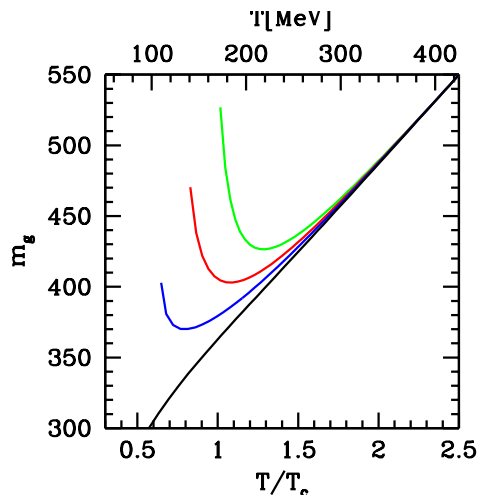


Figure 10: The effective mass of the gluon as a function of T/T_c for various chemical potentials ($\mu_B = 0, 900, 1200$ and 1500 MeV). Upper curves correspond to smaller values of μ_B .

4. Conclusion

In this paper we studied the quasiparticle approach to describe the equation of state of the hot QCD plasma. We have fitted the free parameters of the model by using our 2 + 1 flavor, dynamical staggered QCD lattice results in the region $T, \mu_B < 3T_c$. After calculating the pressure, interaction measure and density we found a good agreement between the quasiparticle predictions and our lattice data. The model successfully justifies the scaling behavior of $\Delta p/\Delta p^{SB}$ observed in the lattice calculations. We gave some confidence intervals for the fit parameters in spite of the lack of continuum extrapolations. Using the best fit parameters the quasiparticle critical line and the speed of sound were given for

higher values of μ_B . The zero temperature limit of the quasiparticle and lattice critical lines (critical μ_B value) cover the $\mu_B^{\text{crit}} \approx 1400 \dots 2000$ MeV region.

Acknowledgements:

We highly appreciate Z. Fodor's continuous help. Useful suggestions on the manuscript from T. Csörgő, B. Kämpfer, S. D. Katz and P. Lévai are also acknowledged. This work was partially supported by Hungarian Scientific grants, OTKA-T34980/T29803/T37615/-M37071/OMFB1548/OMMU-708.

References

- [1] See the proceedings of recent Quark Matter Conferences, Nucl. Phys. A698 (2002), Nucl. Phys. A661 (1999).
- [2] M. G. Alford, K. Rajagopal and F. Wilczek, Phys. Lett. B **422** (1998) 247 [arXiv:hep-ph/9711395]; Nucl. Phys. B **537** (1999) 443 [arXiv:hep-ph/9804403].
- [3] R. Rapp, T. Schafer, E. V. Shuryak and M. Velkovsky, Phys. Rev. Lett. **81** (1998) 53 [arXiv:hep-ph/9711396].
- [4] K. Rajagopal and F. Wilczek, [arXiv:hep-ph/0011333].
- [5] P. Arnold and C. X. Zhai, Phys. Rev. D **50** (1994) 7603 [arXiv:hep-ph/9408276]; Phys. Rev. D **51** (1995) 1906 [arXiv:hep-ph/9410360].
- [6] C. X. Zhai and B. Kastening, Phys. Rev. D **52** (1995) 7232 [arXiv:hep-ph/9507380].
- [7] E. Braaten and A. Nieto, Phys. Rev. D **53** (1996) 3421 [arXiv:hep-ph/9510408].
- [8] F. Karsch, A. Patkós and P. Petreczky, Phys. Lett. B **401** (1997) 69 [arXiv:hep-ph/9702376].
- [9] J. O. Andersen, E. Braaten and M. Strickland, Phys. Rev. D **63** (2001) 105008 [arXiv:hep-ph/0007159].
- [10] J. P. Blaizot, E. Iancu and A. Rebhan, Phys. Rev. Lett. **83** (1999) 2906 [arXiv:hep-ph/9906340]; Phys. Lett. B **470** (1999) 181 [arXiv:hep-ph/9910309]; Phys. Rev. D **63** (2001) 065003 [arXiv:hep-ph/0005003].
- [11] K. Kajantie, M. Laine, K. Rummukainen and Y. Schroder, Phys. Rev. Lett. **86** (2001) 10 [arXiv:hep-ph/0007109].
- [12] S. Gottlieb *et al.*, Phys. Rev. D **55** (1997) 6852 [arXiv:hep-lat/9612020].
- [13] F. Karsch, E. Laermann and A. Peikert, Phys. Lett. B **478** (2000) 447 [arXiv:hep-lat/0002003].
- [14] A. Ali Khan *et al.* [CP-PACS collaboration], Phys. Rev. D **64** (2001) 074510 [arXiv:hep-lat/0103028].
- [15] P. Lévai and U. W. Heinz, Phys. Rev. C **57** (1998) 1879 [arXiv:hep-ph/9710463].
- [16] A. Peshier, B. Kämpfer, G. Soff Phys. Rev. C **61** (2000) 045203 [arXiv:hep-ph/9911474]; Phys. Rev. D **66** (2002) 094003 [arXiv:hep-ph/0206229].
- [17] P. Romatschke [arXiv:hep-ph/0210331].
- [18] Z. Fodor and S. D. Katz, Phys. Lett. B **534** (2002) 87 [arXiv:hep-lat/0104001].

- [19] Z. Fodor and S. D. Katz, JHEP **0203** (2002) 014 [arXiv:hep-lat/0106002].
- [20] C. R. Allton *et al.*, [arXiv:hep-lat/0204010]; S. Ejiri *et al.*, [arXiv:hep-lat/0209012]; C. Schmidt *et al.*, [arXiv:hep-lat/0209009]; C. Schmidt [arXiv:hep-lat/0210037].
- [21] P. de Forcrand and O. Philipsen, [arXiv:hep-lat/0205016]; [arXiv:hep-lat/0209084].
- [22] M. D’Elia and M. P. Lombardo, [arXiv:hep-lat/0205022]; [arXiv:hep-lat/0209146].
- [23] Z. Fodor, S. D. Katz and K. K. Szabó, [arXiv:hep-lat/0208078]; F. Csikor, G. I. Egri, Z. Fodor, S. D. Katz, K. K. Szabó and A. I. Tóth, [arXiv:hep-lat/0209114].
- [24] Z. Fodor, [arXiv:hep-lat/0209101].
- [25] J. Letessier and J. Rafelski, [arXiv:hep-lat/0301099].
- [26] T. D. Lee and S. N. Yang, Phys. Rev. **117** (1960) 22
- [27] W. H. Press, S. A. Teukolsky, W. T. Vetterling and B. P. Flannery 1992, Numerical Recipes in C, 2nd ed. (Cambridge University Press), §15.6; Particle Data Group Phys. Rev. D **66** (2002) 010001.
- [28] A. Andronic, P. Braun-Munzinger, K. Redlich, J. Stachel, [arXiv:nucl-th/0209035]; P. Braun-Munzinger, D. Magestro, K. Redlich, J. Stachel, [arXiv:hep-ph/0105229].
- [29] T. Csörgő, A. Ster, [arXiv:nucl-th/0207016].
- [30] W. Broniowski, W. Florkowski, [arXiv:nucl-th/0204025]; [arXiv:nucl-th/0208061].
- [31] M. Alford, Annu. Rev. Nucl. Part. Sci. **51** (2001) 131-160 [arXiv:hep-ph/0102047].